

Lawrence Berkeley National Laboratory

Lawrence Berkeley National Laboratory

Title

Promises and problems with metallic interconnects for reduced temperature solid oxide fuel cells

Permalink

<https://escholarship.org/uc/item/39b4m2n3>

Authors

Hou, Peggy Y.
Huang, Keqin
Bakker, Wate T.

Publication Date

1999-05-01

PROMISES AND PROBLEMS WITH METALLIC INTERCONNECTS FOR REDUCED TEMPERATURE SOLID OXIDE FUEL CELLS

Peggy Y. Hou, Keqin Huang[†] and Wate T. Bakker*

Materials Sciences Division
Lawrence Berkeley National Laboratory
Berkeley, CA 94720

[†]Texas Materials Institute, ETC 9.102
The University of Texas at Austin
Austin, TX 78713

*Electric Power Research Institute
3412 Hillview Avenue
Palo Alto, CA 94304

ABSTRACT

The oxidation kinetics and electrical properties of oxide scales thermally grown on the surface of a commercial iron-based alloy have been investigated up to 1000°C. The effect of surface coating to improve performance was studied, and it was found that a double coating of Y and Ni oxide was most beneficial. While the Y oxide reduced the oxidation rate, the Ni oxide increased the Cr₂O₃ scale conductivity. Different electrodes were applied to the alloy or to pre-oxidized samples. Some of the electrodes, such as LaSrCoO₃ (LSCo), reacted strongly with the alloy upon oxidation by increasing the oxidation rate and forming a mixed Fe/Co/Cr interlayer that impeded conduction. Application of these electrodes to a pre-oxidized surface eliminated these problems. Preliminary results in reducing atmosphere using Ce_{0.8}+Sm_{0.2}O_{1.9}+Ni and Pt electrodes are also reported. The possibility of using Cr₂O₃ forming alloys as interconnects for low temperature solid oxide fuel cell is discussed in light of these results.

INTRODUCTION

The trend in planar solid oxide fuel cell (SOFC) development is towards lower temperature operation. This has several advantages such as the elimination of interdiffusion between electrodes and electrolytes, ease of internal reforming and the use of relatively low cost metallic interconnects and balance of plant components. Several methods to operate at low temperatures have been identified and demonstrated at a single cell level. The most prominent are the use of thin film, conventional doped zirconia electrolytes (1,2) and the use of a recently discovered new electrolyte, doped lanthanum

gallate (3-6). Since these electrolytes with their associated electrodes have the demonstrated potential to achieve a very low area specific resistance (ASR), generally well below $0.5 \Omega\text{cm}^2$, the electrical resistance of oxide scales on metallic interconnects must be maintained at a very low level over periods of time up to 25,000 hrs to successfully scale up the performance of single cells to fuel cell stacks with multiple metallic interconnects.

High temperature oxidation resistant alloys would appear to be the most appropriate ones for use as interconnects (7-10). Such alloys generally contain chromium and/or aluminum as alloying additives since they form a protective oxide scale by preferential oxidation of chromium to chromia or of aluminum to alumina. Alumina-forming alloys are less interesting for SOFC applications because of the low conductivity of the oxide-scale even though its growth rate is ten times slower than that of Cr_2O_3 . Therefore, numerous studies (7,9,10) have focused on Cr containing Fe or Ni- based alloys that form Cr_2O_3 scale under oxidizing atmospheres at high temperatures since they exhibit a good balance between growth rate and conductivity of the oxide-scale.

Even though Cr containing Fe or Ni based alloys have been shown to be potential candidates as metallic interconnects in SOFCs, many fundamental issues on the electrode/interconnect interfaces need to be resolved before such alloys can be used in practice. These include the interaction of electrode materials with growing oxide scales. Studies on alloy behavior in the anode environment are especially rare.

In this paper we will address oxidation behavior on both the cathode/interconnect and anode/interconnect interfaces. A relatively high purity commercial iron-based alloy was selected because this type of alloy offers a good oxidation resistance as well as a thermal expansion coefficient close to that of the electrolytes used in SOFCs. The study includes oxidation kinetics, microstructural observations, and electrical resistance measurements. Traditional experimental techniques such as thermogravimetry, X-ray diffraction, SEM/EDS, and two-probe resistance measurements were used.

EXPERIMENTAL PROCEDURES

Table 1: Alloy Composition in Weight %

C	Mn	P	S	Si	Cr	Ni	Al	Mo	Cu	Cd	Ti	N	Co	V	Fe
0.02	0.1	0.01	0.01	0.21	26.3	0.15	0.05	1.01	0.05	0.12	0.05	0.01	0.05	0.01	bal

A commercial Fe-based alloy, whose composition is given in Table 1, was used for this study. The as-received 1 mm sheet was cut into 1 cm x 1 cm square plates, then polished with SiC sand paper to a 1200 grit finish. Oxidation was carried out in stagnant air either in a Cahn microbalance for rate measurement or in a horizontal tube furnace in alumina boats.

Application of surface yttrium and nickel oxides prior to oxidation was achieved by the hot-dipping method described by Hou et al. (11). After a short low temperature pre-oxidation step, the specimen was quickly inserted into an aqueous nitrate solution of

the desired salt, then heated in air at 500°C to decompose the nitrate into oxide. Co-deposition of Y and Ni oxides was achieved by dipping in a mixture of the two nitrate solutions. Deposition of different cathode materials, such as LSCo ($\text{La}_{0.6}\text{Sr}_{0.4}\text{CoO}_3$), LSM ($\text{La}_{0.85}\text{Sr}_{0.15}\text{MnO}_3$) + LSGM ($\text{La}_{0.80}\text{Sr}_{0.20}\text{Ga}_{0.83}\text{Mg}_{0.17}\text{O}_{2.85}$) and Pt, was done by painting the electrodes on unoxidized or pre-oxidized specimens. To avoid extensive oxidation of the alloy, the electrodes were not calcined, but were tested directly at the oxidation temperature.

Electrical resistance measurements were conducted using a 2-point probe method as shown in Figure 1. Assuming zero resistance through the alloy, the method measures the resistance of the oxide scale and of all interfaces. A constant current of 10 mA was used and the voltage across the sample was measured with a multimeter. Different currents had been used initially to establish the fact that the system exhibits ohmic behavior. The Pt meshes were placed onto the test sample using Pt paste and the wires were spot welded onto the mesh. The test assembly was placed in a furnace and heated. Measurements usually started at 600°C and continued with every 50 or 100°C increment up to the oxidation temperature. The dwell time at each temperature was no more than 30 minutes and the conductivity during this time was normally constant. Similar measurements were also taken during cooling. For long term testing, the sample would be heated and held at the desired temperature while the change in electrical property was determined as a function of time. The behavior in reducing atmosphere was studied in 3% H_2O mixed in H_2 , with Pt or $\text{Ce}_{0.8}\text{Sm}_{0.2}\text{O}_{1.9}$ + NiO (40:60 in weight percent) as the electrode.

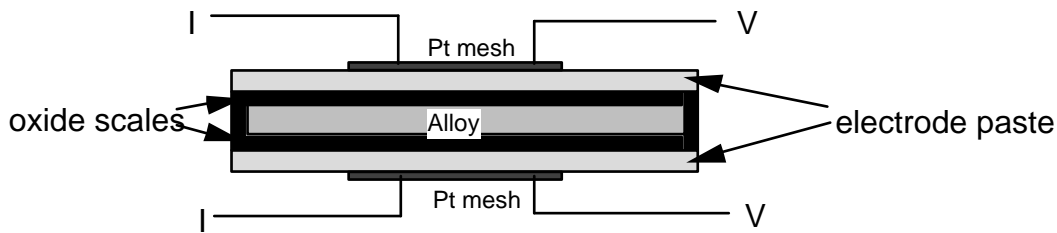


Figure 1 Experimental setup for ASR measurements

Selected specimens were characterized using X-ray diffraction to determine the type of oxide that formed. Scanning electron microscopy (SEM) equipped with an energy dispersive X-ray analyzer (EDS) was used to examine the specimen surface and polished cross-sections to study the morphology and chemical distribution of the various components. Particular focus was placed on the electrode/scale and the scale/alloy interfaces.

RESULTS AND DISCUSSION

Alloy Behavior in Air

Near parabolic oxidation behavior was observed at all the test temperatures,

between 800-1000°C, after an initial transient stage. From the temperature dependence, the activation energy was determined to be 2.3 eV. X-ray diffraction analysis showed that the oxide scale was Cr₂O₃. Using the density of bulk Cr₂O₃, the parabolic rate constant obtained by weight gain could be converted to a thickness change. These values are comparable to Cr₂O₃ growth rates reported in the literature (12), and are given in Table 2. Spallation of the scale occurred during cooling after it thickened to ≥ 1 μm, which could be a problem in long term operation under thermal cycling conditions. Oxidation in H₂O saturated air (about 2.3%) showed similar behavior, indicating that this alloy is rather resistant to the detrimental effect of moisture that is sometimes associated with scale growth (13).

Table 2: Parabolic rate constants in air at different temperatures

Temperature (°C)	k_g (g ² cm ⁻⁴ s ⁻¹)	k_p (μm/h ^{1/2})
800	8.8×10^{-14}	0.108
850	$(2.2-3.1) \times 10^{-13}$	0.188
900	$(9.5-9.7) \times 10^{-13}$	0.358
1000	3.1×10^{-12}	0.643

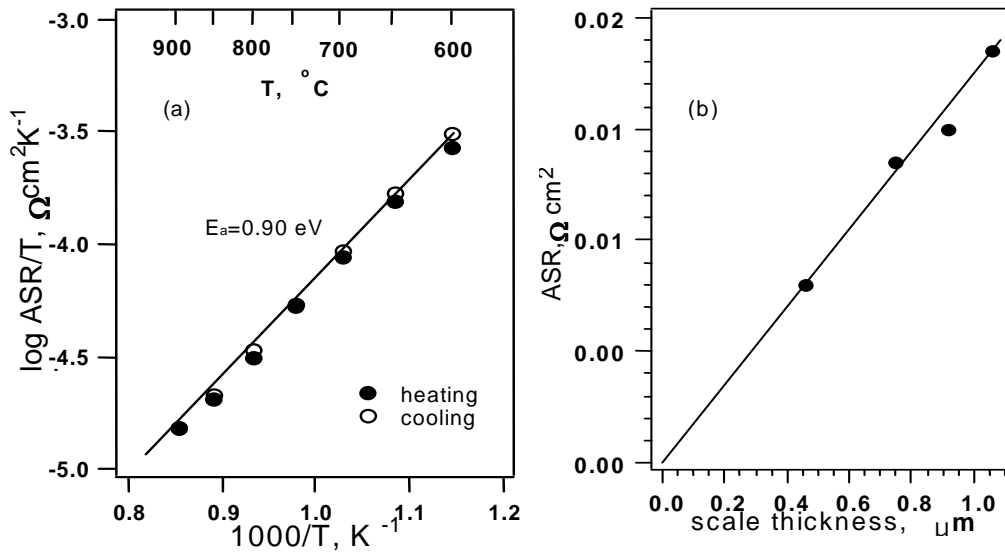


Figure 2: (a) ASR of Cr₂O₃ scale (formed by preoxidation at 900°C for 24 hours) as a function of temperature, measured during heating and cooling using Pt electrode. (b) ASR as a function of scale thickness at 800°C.

Conductivity of the Cr₂O₃ scale determined using Pt electrode is given in Figure 2. From Fig. 2(a), the measurement is seen to be consistent and reproducible during heating and cooling, and the activation energy was about 0.9 eV. This value is lower than what would be expected for single crystal Cr₂O₃ (14) indicating extrinsic behavior, where the conductivity is dominated by impurities in the Cr₂O₃ scale. It is not surprising that the

Cr₂O₃ scale formed on an alloy would contain a high level of impurities, especially the major alloying element, in this case Fe.

The change in ASR with scale thickness was determined using different samples oxidized at 800°C after different times. The result in Fig. 2(b) shows a linear relationship as expected from Ohm's law, which indicates negligible interfacial resistance as a function of scale growth. The greatest resistance is from the scale itself.

With the relationship of the scale growth rate and the ASR established as a function of time and temperature, we can predict the long-term behavior of these systems for any operating conditions.

Since scale thickness $l = k_p/\sqrt{t} = [k_o \exp(-E_{ox}/kT)] / \sqrt{t}$, where k_p is the parabolic rate constant, t is time and T is temperature in degree K, and $ASR = l / \sigma = l / [(\sigma_o/T) \exp(-E_{el}/kT)]$,

$$ASR = \frac{\sqrt{k_p t}}{\sigma} = \frac{\sqrt{k_o t}}{\sigma_o} T \exp\left(\frac{-1/2E_{ox} + E_{el}}{kT}\right) \quad [1]$$

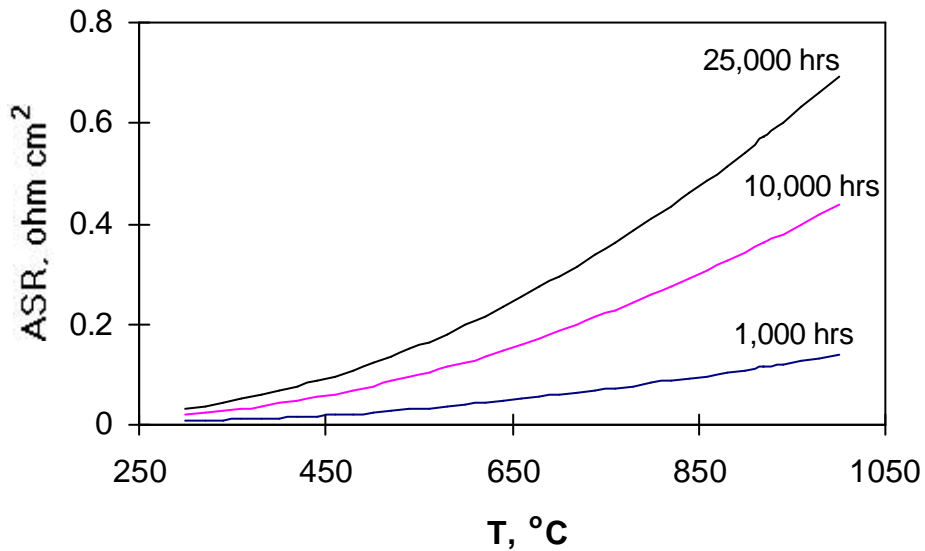


Figure 3: Prediction of the effect of temperature on ASR under scale growth condition.

The equation attests that ASR increases with time in a parabolic fashion. The relationship of ASR and temperature depends on the relative activation energies of the oxidation and the conductivity processes. Using the experimental values from our study, the change in ASR with temperature is plotted in Figure 3. Surprisingly, the ASR value continuously increased with temperature, even though the resistance of a bulk oxide is expected to decrease at higher temperatures (14). The observed behavior is an indication that oxidation rate is dominating, such that the resulting ASR value becomes dictated by the scale thickness that forms under a given temperature. The key to reducing the ASR, therefore, is to operate at the lowest possible temperature and to decrease the oxidation rate. Any method that would cause an increase in the scale conductivity would certainly be beneficial as well.

Effect of Surface Dopants

One well-known phenomenon in high temperature oxidation is that the addition of reactive elements, such as Y, Ce and La, to Cr_2O_3 and Al_2O_3 forming alloys can greatly reduce the oxidation rate and increase the scale adhesion at temperatures above 900°C (15,16). There are also studies showing that these elements are equally effective when added as a surface coating (17,18). What is not known, however, is whether the beneficial effect can be observed at reduced temperatures below 900°C . Several different reactive element nitrates have been tested to study their effect on Cr_2O_3 scale growth, and it was found that Y was the most effective. Although its benefit at 800°C was not as great as it would be at higher temperatures, a more than two-fold reduction in growth rate was still achieved, as seen in Figure 4 and Table 3. This reduction should lower the total ASR by the same factor, since the oxidation activation energy was not changed by the applied Y. The ASR after 25,000 hrs at 800°C (Fig. 3) could then be reduced to less than $0.2 \Omega\text{cm}^2$, which would be more compatible to the cell resistance.

Surface coating with NiO did not affect the oxidation and co-doping of Y and Ni oxides gave the dominant effect of the Y. The reason to study the effect of NiO coating was an attempt to incorporate Ni^{2+} ions into the Cr_2O_3 scale to increase its conductivity.

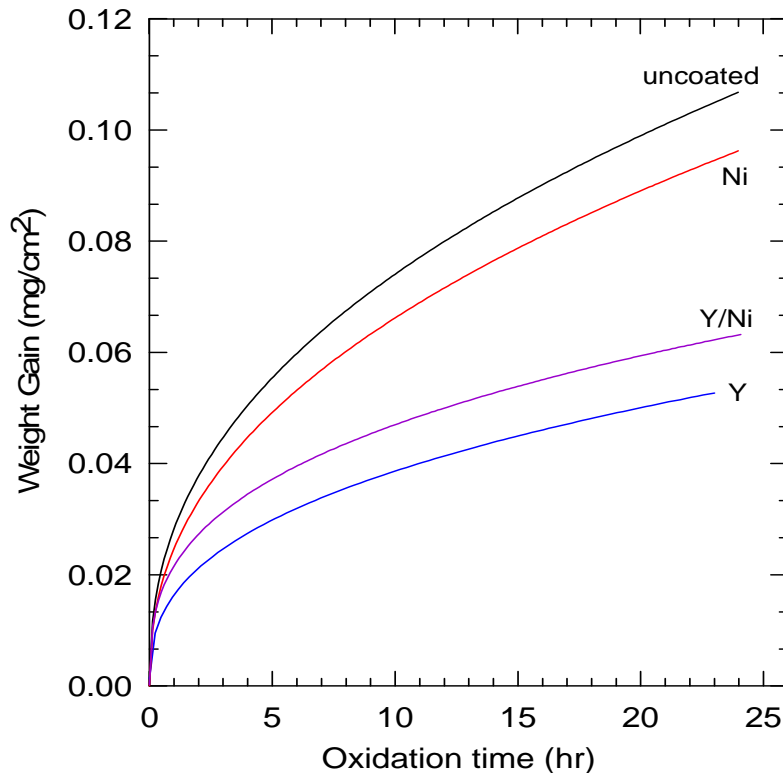


Figure 4: Effect of different surface oxide coatings on the oxidation rate at 800°C .

Table 3: Effect of surface dopants on parabolic rate constants at 800°C

Type of surface coating	k_g ($\text{g}^2 \text{cm}^{-4} \text{s}^{-1}$)	k_p ($\mu\text{m}/\text{h}^{1/2}$)
uncoated	8.8×10^{-14}	0.108
Ni	9.1×10^{-14}	0.110
Y	3.3×10^{-14}	0.066
Y/Ni	3.4×10^{-14}	0.067

The effects of Y, Ni and Y/Ni surface thin coatings on the conductivity of the oxide scales are shown in Figure 5. The slight reduction with the Y coating should be a result of the scale being thinner, and probably also due to a more defect-free scale and a more adherent scale/alloy interface (18). The Ni coating showed rather pronounced reduction in ASR, which further demonstrates that the conductivity behavior is extrinsic, where the lower valence Ni^{2+} cation increases the hole concentration in Cr_2O_3 . This behavior is similar to the observed increase in conductivity when a few mole% of NiO was added to sintered Cr_2O_3 (19,20). Co-doping of Ni and Y further reduced the ASR. Combining the beneficial effect of Ni on conductivity to that of Y on the oxidation rate, the predicted ASR (Fig. 3) after 25,000 hrs at 800°C could be reduced to as low as $0.05 \Omega\text{cm}^2$. This promising behavior suggests that future alloys should contain small amounts of Y, and perhaps Ni-based instead of Fe-based alloys will be a better choice. However, Fe-based alloys usually have more compatible thermal expansion coefficients with the ceramic cell components.

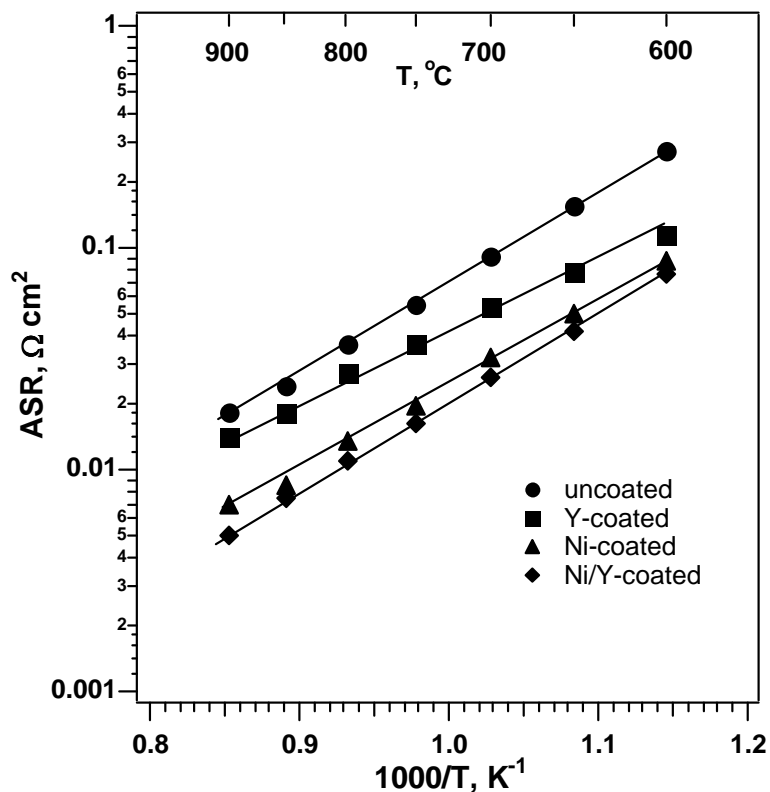


Figure 5: Comparison of ASR with different surface coatings as a function of temperature.

Effect of Electrode Materials

Since the metallic interconnect will be in direct contact with the ceramic electrode material, it is important to understand the interaction between them, if any. The effect of three different electrodes on the oxidation kinetics is shown in Figure 6. In all cases, the suspended electrodes were simply painted onto the specimen surface without further heat-treatment, except for the Pt paint, which was heated at 800°C for 0.5 hr before oxidation. Of all the electrodes tested, LSM+LSGM showed no effect on scale growth. LSCo increased the oxidation rate, especially at the initial stage. It is not yet clear how and why the LSCo would enhance the oxidation rate. Possibly, the fast rate was associated with faster growing oxides, such as Fe_2O_3 , or some mixed spinels. Pt reduced the rate at later time, where scale growth is in the parabolic regime. This beneficial effect of Pt is similar to that of reactive elements, such as Y, and has been reported, particularly for Al_2O_3 forming alloys and/or coatings (21).

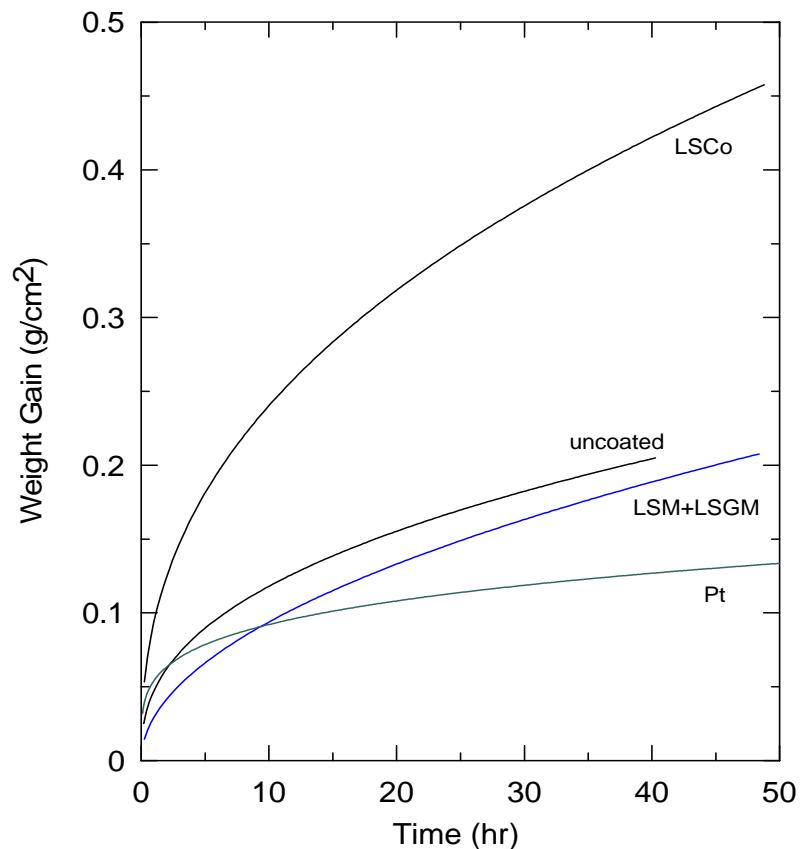


Figure 6: Effect of different electrode materials on the oxidation kinetics at 850°C.

The effect of the deposited electrodes on ASR as a function of time at 850°C is presented in Figure 7. Similar to the oxidation study, the electrodes were deposited directly onto the alloy surface. Pt is seen to yield the lowest ASR with a parabolic dependence on time, which implies that the growth of the scale thickness causes the increase of the ASR. The LSM+LSGM electrode had an intermediate ASR value that slightly deviated from parabolic behavior. With LSCo, the ASR values increased dramatically with time and deviated significantly from a parabolic dependence. This high

value is partially due to the enhanced oxidation rate, as seen in Fig. 6, partially due to an expected high interface contact from the loosely bonded electrode and partially due to the formation of a mixed Co, Fe and Cr-rich region that is porous. From cross-sectional examination using EDS and SEM, this region was found either at the Cr_2O_3 /cathode interface or was directly in contact with the alloy, indicating some interaction of the cathode material with the alloy surface to form mixed oxides. Similar Mn and Cr-rich regions were found on the LSM+LSGM coated sample, except that the width was only half that compared to those found on the LSCo coated sample. The detrimental effect on conductivity due to porous spinel formation between the ceramic electrode and the alloy or with the Cr_2O_3 scale under long term operations (9) should be studied in more detail, so that proper choices of the interconnect and the electrode can be made to eliminate this problem.

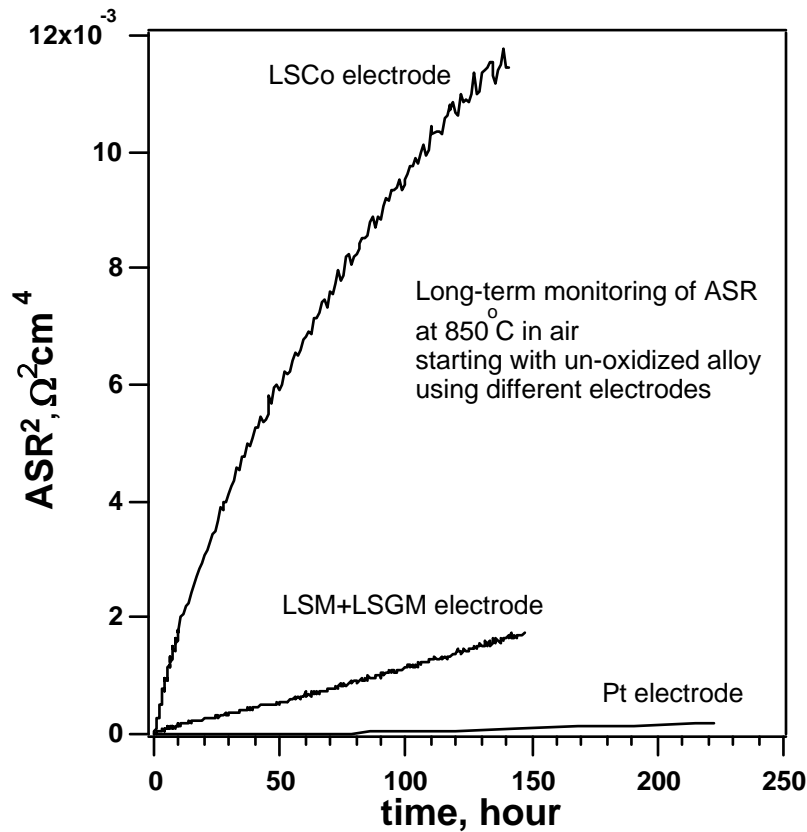


Figure 7: Dependence of ASR^2 with time measured at 850°C in air with three different electrodes on the surface of un-oxidized alloys.

On a pre-oxidized alloy, Fig. 8, the detrimental effect of LSCo becomes much less. After an initially rapid increase, the ASR saturated and remained rather constant. Similar behavior is seen with the LSM+LSGM electrode, except that the ASR value is higher. When Pt was used, the ASR remained less than $0.05 \Omega\text{cm}^2$, which is close to the predicted $0.03 \Omega\text{cm}^2$ after 100 hours based on Eqn. 1. The reason for the ASR decrease after 100 hours is not known, but may be caused by some Pt penetration through the Cr_2O_3 scale. With the ceramic electrodes, instead of measuring the ASR increase as a function of scale growth, which should be parabolic, the saturated high ASR values indicate a dominance of interface resistance. This is most likely caused by the poor

bonding of the ceramic electrode to the alloy surface. Since these materials were only painted onto the alloy without any further heat treatment, it is expected that they would produce a high interface resistance, especially during the initial stage. Application of some pressure during this kind of testing may decrease this resistance, therefore, provide more realistic values. Such experiments are currently underway. Other methods of applying the oxide electrodes, such as spray coating used by Kadowaki et al (22), may also be more desirable. In their study, the ASR only changed slightly, decreasing on one alloy and increasing on the other, with prolonged oxidation.

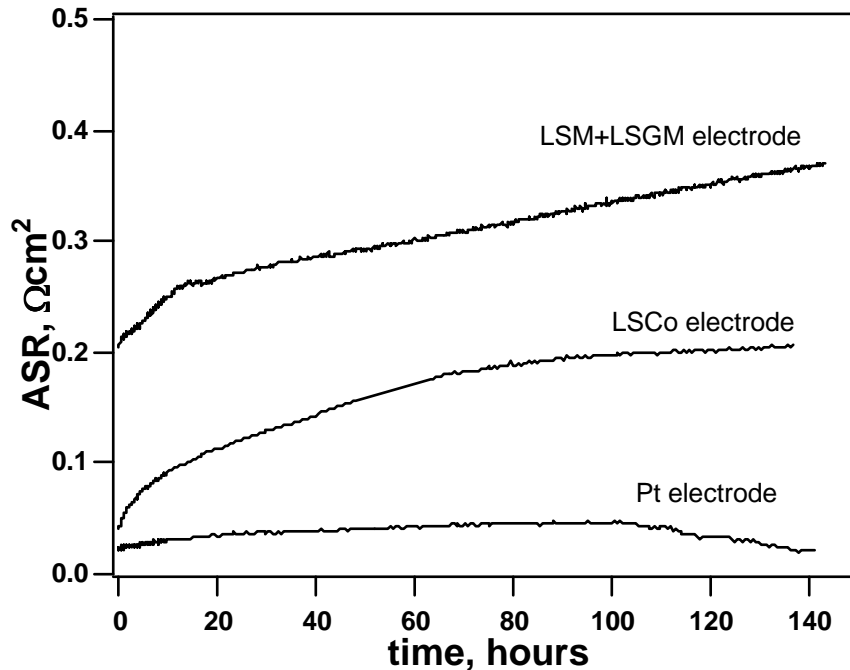


Figure 8: Dependence of ASR on time measured at 850°C in air with alloy pre-oxidized at 900°C for 24 hours using different electrodes.

Performance in Reducing Atmosphere

There has been little reported study on the behavior of metallic interconnects under the anode environment. Our preliminary results tested under $H_2+3\% H_2O$ using Pt and CS20+Ni electrodes are shown in Figure 9. Fairly high initial ASR values were obtained with the CS20+Ni electrode. The rapid decrease with time reflects a gradual reduction of NiO to Ni that improves the electrode conduction. For both the Pt and the CS20+Ni, their ASR remains almost unchanged with time after this initial period, which implies a very slow oxidation rate and a stable interface. Provided that scale growth is the same for both electrodes, the interfacial resistance of CS20+Ni/ Cr_2O_3 should be about three times higher than that of Pt/ Cr_2O_3 . The higher ASR even with the Pt electrode when compared with those tested in air shows that interface resistance is greater at the anode side than at the cathode side. The reason is not clear and the fact that the ASR level remained constant throughout the duration of the 150 hr test requires further study.

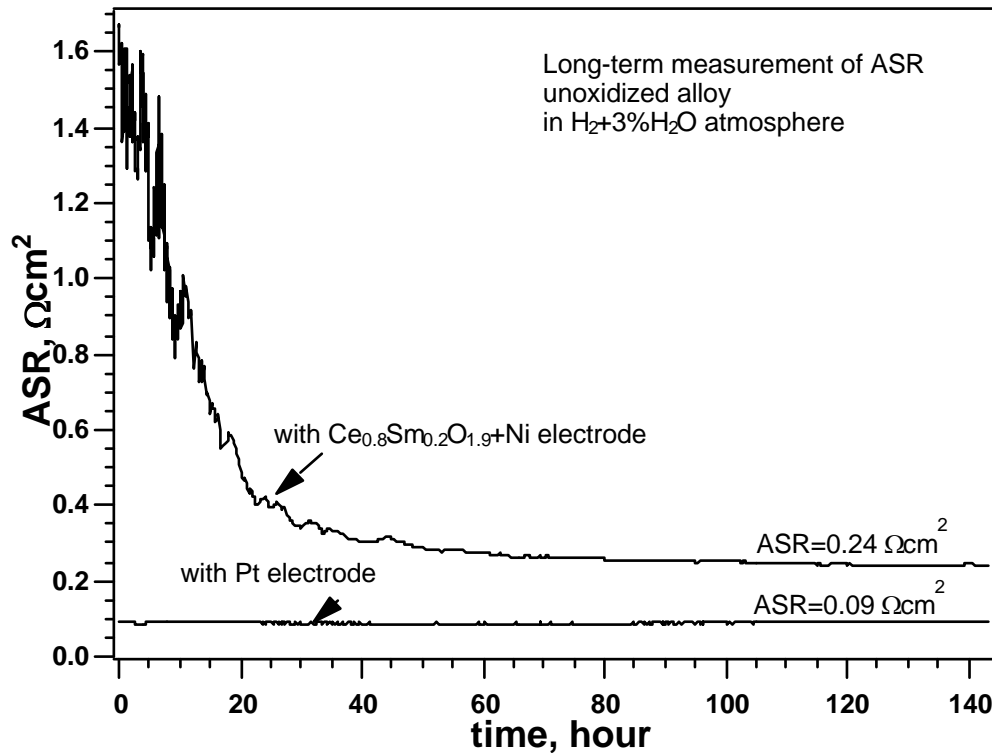


Figure 9: Dependence of ASR on time measured at 850°C in H₂+3%H₂O atmosphere with different electrodes on the surface of un-oxidized alloys

CONCLUSIONS

- The oxide growth rate is the major factor limiting alloy performance as interconnect materials in SOFC's at all temperatures. Thus SOFC's with metal interconnects should be operated at the lowest temperature, where the total system will provide the desired power density and efficiency.
- Reduction of the oxide growth rate can be achieved by the addition of reactive element, such as Y, which can be applied as a thin surface oxide coating. Co-depositing the Y oxide with NiO further improves the alloy performance by increasing the Cr₂O₃ scale conductivity due to the incorporation of the lower valence Ni²⁺ cation in the Cr₂O₃ scale.
- Application of ceramic electrodes directly unto alloy surfaces appears to increase the overall system resistance significantly, probably because of the formation of low conductivity interfacial layers. Pre-oxidation of the alloy to form a thin layer of Cr₂O₃ scale, thus separating the electrode from the alloy surface, avoids much of the problem. However, it is still a challenge to ensure good bonding between the electrode and the interconnect without severely oxidizing the interconnect at elevated temperatures, such as to minimize interfacial contact resistance.
- The Cr₂O₃ scale resistance under a reduced atmosphere of H₂/H₂O as found on the anode side seems to be significantly higher than that found on the cathode side.

Further evaluation is needed.

ACKNOWLEDGMENTS

This work was supported by the Electric Power Research Institute under project WO8602-13 through an agreement with the U.S. Department of Energy, contract no. DE-AC03-76SF00098.

REFERENCES

1. S. de Souza, S. J. Visco and L. C. De Jonghe, *Solid State Ionics* **98**, 571 (1997).
2. S. de Souza, S. J. Visco and L. C. De Jonghe, *J. Electrochem. Soc.* **144**, L35 (1997).
3. H. Ishihara, H. Matsuda and Y. Takita, *J. Am. Chem. Soc.*, **116**, 3801 (1994).
4. M. Feng and J. B. Goodenough, *Eur. J. Solid State Inorg. Chem.*, **T31**, 663 (1994).
5. P. Huang and A. Petric, *J. Electrochem. Soc.*, **143** (5), 1644 (1996).
6. K. Q. Huang, R. Tichy and J. B. Goodenough, *J. Am. Ceram. Soc.*, **81**, 2565 (1998).
7. W. J. Quadackers, H. Greiner and W. Kock, in *Proceedings of Ist European SOFC Forum*, U. Bossel, Editor, p. 525, Lucerne, Switzerland (1994).
8. P. Kofstad and R. Bredesen, *Solid State Ionics* **52**, 69 (1992).
9. W. J. Quadackers, H. Greiner, M. Hansel, A. Pattanaik, A.S. Khanna, W. Mallener, *Solid State Ionics*, **91**, 55 (1996).
10. S. Linderoth, P. V. Hendriksen and m. Mogensen, *J. Mat. Sci.* **31**, 5077 (1996).
11. P. Y. Hou and J. Stringer, *J. Electrochem. Soc.*, **134**, 1836 (1987).
12. H. Hindam and D. P. Whittle, *Oxid. Met.*, **18**, 245 (1982).
13. D. L. Douglass, P. Kofstad, A. Rahmel and G. C. Wood, *Oxid. Met.*, **45**, 529 (1996).
14. P. Kofstad, *Nonstoichiometry, Diffusion, and Electrical Conductivity in Binary Metal Oxides*, p.204, Wiley-Interscience, New York (1972).
15. L. B. Pfeil, U.K. Patent No. 459848, 1937.
16. D. P. Whittle and J. Stringer, *Phil. Trans. R. Soc. Lond.*, **A27**, 309 (1979).
17. L. B. Pfeil, U.K. Patent No. 574088, 1945.
18. P. Y. Hou and J. Stringer, *Mater. Sci. Eng.*, **A202**, 1 (1995).
19. W. A. Fisher and G. Lorenz, *Arch. Eisenhüttenw.*, **28**, 497 (1957).
20. K. Hauffe and J. Block, *Z. Phys. Chem.*, **198**, 232 (1951).
21. G. R. Krishna, D. K. Das, V. Singh and S. V. Joshi, *Mater. Sci Eng. A.*, **251**, 40 (1998).
22. T. Kadowaki, T. Shiomitsu, E. Matsuda, H. Nakagawa and H. Tsuneizumi, *Solid State Ionics*, **67**, 65 (1993).